Electronic Supplementary Material (ESI) for ChemComm.


# Supplementary Information

# Chemically-induced redox switching of a metalloprotein reveals thermodynamic and kinetic heterogeneity, one molecule at a time

**Namik Akkilic*, Fenna van der Grient, Muhammad Kamran, Nusrat J.M. Sanghamitra**

Leiden Institute of Physics, Huygens Laboratory, Leiden University, Niels Bohrweg 2, 2333CA Leiden, The Netherlands

*Address correspondence: akkilic@physics.leidenuniv.nl

## Supplementary Methods:

**Azurin Purification and Labeling.** Wild type azurin from *Pseudomonas aeruginosa* was expressed in *E. coli* and purified as previously described.[1] Protein labeling was performed using a slightly modified version of a previously described protocol.[2] Azurin was incubated in a molar ratio of 1:1 with the NHS-ester of the fluorescent label Cy5 (GE Healthcare, UK) in 20 mM HEPES buffer pH 8.3, for 2 hours as recommended by the manufacturers for N-terminal labeling. The unreacted label was then removed using a 5 ml HiTrap Desalting column (GE Healthcare). During the desalting step a buffer exchange to 5 mM Tris/HCl pH 8.5 was performed for the purification step. According to the matrix–assisted laser desorption ionization (MALDI) analysis,[2] we assume that Cy5 NHS–ester reacts mainly with the N terminal –NH2 of azurin.

**Purification of labeled species.** Ion exchange chromatography (IEC) of the labeled protein species was performed on a 1 ml MonoQ column (GE Healthcare) using an Äkta Purifier (GE Healthcare) system. The labeled azurin fraction was loaded on the column (equilibrated with 5mM Tris pH 8.5) and subsequently protein species were eluted with a gradient from 0 to 100 mM NaCl in 5mM Tris pH 8.5 in 30 column volumes at a flow rate of 1 ml/min as recommended by the manufacturer. The elution process was followed by monitoring the absorbance at 280 nm (azurin) and 650 nm (characteristic absorption of Cy5) as shown in Figure S3. The fractions corresponding to each peak were then collected and checked by means of UV/Vis spectroscopy to confirm the presence of protein.

**Absorption and Fluorescence Spectroscopy.** Absorption spectra were measured using a Perkin Elmer Instruments Lambda 800 spectrophotometer with a slit width equivalent to a bandwidth of 2 nm. Fluorescence spectra and time courses in bulk were measured with an LS 55 commercial fluorimeter (Perkin Elmer, USA), with a red sensitive photo–multiplier (R928, Hamamatsu, Japan), set to 5 nm band pass. Cy5 fluorescence was excited at 645 nm, and the fluorescence intensity at 665 nm was used for the analysis of the switching efficiency.

To verify redox changes in bulk solution, fluorescence time courses were measured in a 5x5 mm quartz cuvette (Perkin Elmer) in 100 mM phosphate buffer at pH 7.0 buffer solution. The Cy5 concentration was 100 nM. Protein reduction and oxidation during measurement was performed by adding reductants (dithiotreitol, DTT) and oxidant (potassium ferricyanide, $K_3(FeCN)_6$) from

freshly prepared concentrated stock solutions (2–20 mM) directly into the cuvette to a final concentration of 5-20 μM, i.e. in 50 to 200–fold excess.

**Covalent attachment of azurin on glass.** All glass slides were MENZEL GLÄSER Nr. 1 (Gerhard Menzel GmbH, Germany) which were cleaned by sonication in spectrometer grade acetone (45 min), then dipped in 10% $NaOH/H_2O$ (45 min) and finally stored in methanol. Between each step, the slides were thoroughly rinsed and sonicated in deionized water (MilliQ). Before use the cover slips were blow dried under $N_2$ flow and ozone–cleaned (UVP PR–100 UV–ozone photoreactor) for 1 h immediately before silanization. The surface of the cleaned glass slides was modified by depositing a layer of a 4:1 mixture of triethoxysilane (TES) and mercaptopropyl trimethoxysilane (MPTS) (see Scheme 1)[3,4] All the silanes were purchased from Fluka and used without purification. In the second step, Succinimidyl–[(N-maleimidopropionamido)–hexaethyleneglycol] ester) (NHS–$PEO_4$–Maleimide, Pierce) was covalently bound to one of the Lys on the wt–azurin labeled with Cy5. According to the instructions from the manufacturer, NHS–$PEO_4$–Maleimide linker was added to a 100–fold excess of the protein in 20 mM HEPES buffer pH 8.3. After 1 hour the excess of the linker was then removed using a Centrispin–10 size exclusion column with a 5–kDa cut–off (Princeton separations, Adelphia, NJ, USA).[3] Finally, the 100 pM of NHS–$PEO_4$–Maleimide modified azurin–Cy5 in 20 mM HEPES buffer pH 7.0 was incubated on silanized glass slide for overnight at 4 ℃ and then rinsed with 10 mM potassium phosphate buffer at pH 7.0 to remove free azurin. In the last step, the maleimide–end of the linker is attached to the exposed thiols at the silanized glass surface. This gave reproducible results of specifically immobilized individual wt–azurin molecules at the glass surface.

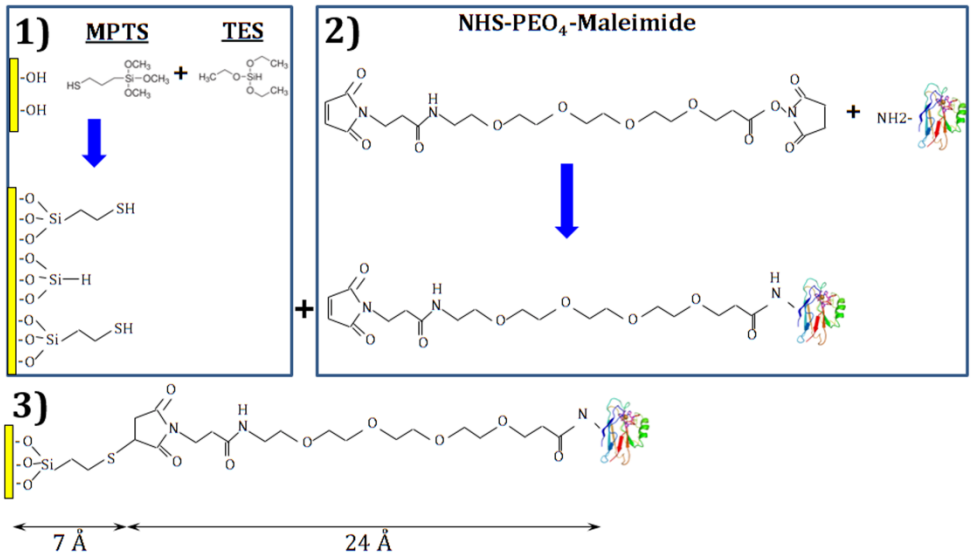


**Scheme 1:** Protein immobilization in 3 steps: In step 1, glass slides were modified by depositing a layer of a 4:1 mixture of TES/MPTS with −SH groups exposed at the surface. Separately, in step 2, the NHS-$PEO_4$-maleimide linker is covalently bound to ε -NH2 of lysine on the wt–azurin. Finally, the maleimide–end of the latter construct is attached to the exposed thiols at the silanized glass surface via the 24 Å long linker. The overall length of the linkers between the surface and the protein is about 31 Å.

**Single molecule imaging setup and single photon counting.** The single molecule fluorescence measurements were conducted on a home–built sample scanning confocal microscope. The scanning confocal microscope was equipped with Time–Correlated Single–Photon Counting (TCSPC) capabilities. For fluorescence excitation a pulsed picosecond diode laser with 40 MHz repetition rate (PDL 800–B, PicoQuant GmbH) and an output wavelength of 639 nm was sent through a narrow–band clean–up filter (LD01–640/8–25, Semrock, USA), then coupled into a single–mode optical fiber, the output of which was collimated using a telescope system made of two achromatic lenses (+60 mm and +40 mm). The collimated beam was directed into the back entrance of an Axiovert 100 microscope (Zeiss), reflected by a dichroic mirror (Z 532/633 M, Chroma technology, USA) to a high numerical aperture (NA) oil objective (100× oil, NA 1.4, Zeiss, Germany) and then focused to a diffraction–limited spot (~300 nm) on the sample surface (Fig. S9). A power density of ~0.4 kW/$cm^2$ was used at the sample to avoid excessive bleaching while recording fluorescence time traces. Epi–fluorescence from the labeled azurin was filtered

with an emission filter (D 675/50 M, Chroma technology, USA) and focused with a +80 mm focal length achromatic lens on to the active area of a single photon avalanche photodiode (Perkin–Elmer SPCM–AQR–14). The data acquisition was performed by the TimeHarp 200 TCSPC PC-board (PicoQuant, GmbH) operating in the special Time–Tagged Time–Resolved (T3R) mode, which stores the arrival time of each individual photon event. Samples were mounted onto a P–517 nanopositioner which was connected to an E–71 control unit; both from Physik Instrumente Gmbh. Scanning, accurate positioning and data collection were performed by the SymPhoTime software package (PicoQuant GmbH). Fluorescence images were acquired by scanning a 10 × 10 $\mu m^2$ area of the sample on the glass surface with a step size of 100 nm and a dwell time of 2 ms per point. A characteristic sample scanning confocal image is shown in Figure 1B. After imaging, the molecules in the scanned area were manually selected and an automatic recording procedure was started. During this procedure the scanner was moved successively to each selected spot and the fluorescence time trace was recorded over a time interval of up to 60 seconds before moving on to the next spot until all the selected spots had been processed. The fluorescence recorded from each single molecule was stored in a file to be further elaborated off–line.

**Redox potential of buffer solution.** Single molecule detection was performed in 100 mM phosphate buffer solution at pH 7.0 with freshly prepared $K_3(FeCN)_6$ and DTT as oxidant and reductant (Fig. 1A), respectively. The chemical redox potential of the buffer solution ($E$) in single molecule experiments was varied around the midpoint potential of azurin by adjusting the relative concentration of $K_3(FeCN)_6$ and DTT. The initial concentration of the $K_3(FeCN)_6$ was 200 μM in all cases and DTT was added to reach the final potentials of −20, 0, 20, 40, 60, 80 and 100 mV. The potential of the solution was measured with a voltmeter using a saturated calomel electrode (SCE) as a reference (RE) and 0.5 mm platinum wire as a counter electrode (CE). All the measurements were performed in anaerobic conditions in a sealed sample–holder under continuous argon flow.

In the measurements on Cy5–labeled azurin, it proved, indeed, essential to remove oxygen from the solution. Adding oxygen scavengers to the solution was not an option because they may interact with the label or the chemicals in solution. Moreover, triplet state quenchers (e.g., Trolox, β-mercaptoethylamine) have key limitations, including poor aqueous solubility,

problems with membrane permeability and biological toxicity.[5] Rather, oxygen was removed by sparging with argon. It dramatically increased the number of emitted photons from the Cy5–label before bleaching. Under those conditions, and with 100–200 μM of reductant and oxidant in solution, we did not see any blinking in the control experiments with Cy5–labeled Zn-Az on the millisecond time scale (Fig. S5). We can actually not exclude that blinking still occurs on the sub–millisecond time scale. It is quite possible that the redox components in solution contribute to triplet quenching and the suppression of subsequent photochemical reactions of Cy5 labeled azurin. The conjugation of Cy5 with azurin is also likely to reduce the propensity for photoisomerization.

**Data elaboration and analysis.** The files containing the time–tagged time–resolved data were converted to ASCII format, and processed using a change point (CP) –finding algorithm implemented in software which was kindly provided by Dr. Haw Yang, Princeton University.[6] In essence, this CP program uses a generalized likelihood ratio test that determines the location of an intensity change point based on individual photon arrival times without the artificial time resolution limitations that arise from binning and thresholding. The CP analyses were actually performed in terms of 5 intensity levels, because then we were able to reliably identify the occasional blinking event by the intensity drop to the background level. The CP–finding algorithm was run using a parameter value of $\alpha = 0.01$ for Type I errors (false positive) and a confidence parameter value of $\beta = 0.95$ to set the confidence interval around each change point. The output of the CP–finding algorithm was further elaborated by using a home written algorithm to determine the time intervals associated with the oxidized (off) and the reduced state (on), respectively. Only traces longer than 0.5 second and showing at least 2 transitions between different states (fluorescence on and off) were taken into account for further analysis. The *in–bulk* switching ratio was used as a threshold criterion to discriminate on times (above the threshold) and off times (below the threshold). In particular, the condition for a state change was imposed such that the intensity ratio before and after fell within ±2.5 standard deviations of the in-bulk switching ratio (99% confidence interval around the mean). Intensity drops to the background level due to blinking events were distinguished by assuming that the intensity of the oxidized state is at least a factor of 1.2 higher than the background level. Such blinking events were not counted as state changes. The time that a molecule stays in oxidized (reduced) state, on

(off) time, from the selected single molecules were stored and subsequently analyzed. Data analysis was performed using custom–written algorithms on Matlab 7.9.

Fitting of the on- and off-times histogram was performed with a mono-exponential function defined as follows:

$$y = y_0 e^{-kx} \tag{1}$$

where $x$ is the time bin number and $y$ is its occurrence. The fitted parameters are: $y_0$, the $y$ value at time zero and $k$, the rate constant of the decay. According to which distribution was fitted, a ‘‘on’’ or ‘‘off’’ subscript was added to $k$, corresponding to the reduced and oxidized state of azurin, respectively, to distinguish the two parameters.

The parameter $P_{ox}$ ($P_{red}$) is used in the present work to describe the time–averaged probability that the molecule is in the oxidized (reduced) state.[7] The value of $P_{ox}$ for each time trace was calculated as follows:

$$P_{ox} = \frac{\sum_{i=1}^{n} \tau_{i,off}}{\sum_{i=1}^{n} \tau_{i,off} + \sum_{j=1}^{m} \tau_{j,on}} \tag{2}$$

where $\tau_{i,off}$ and $\tau_{j,on}$ are the *i*–th off– and *j*–th on–times, respectively; *n* and *m* are the total number of off– and on–time intervals in a single trace, respectively. A similar expression is used to calculate $P_{red}$. The denominator is essentially the total duration of the time trace (before bleaching).

**Redox thermodynamics of single molecules**

**The Nernst equation.** The electrode potential of a redox couple in solutions, i.e. the free energy when referenced against a standard hydrogen electrode (SHE), is given by the Nernst equation in terms of the concentrations of reductant and oxidant ([*red*] and [*ox*], respectively),

$$E = E_0 - \frac{RT}{nF} \ln \frac{[red]}{[ox]} \quad (3)$$

Here, $R$ is the universal gas constant ($R = 8.314\,472\,J\,K^{-1}\,mol^{-1}$), $T$ is the absolute temperature, and $E_0$ is the midpoint potential of the reaction. $F$ is the Faraday constant ($F = 9.648\,53399 \times 10^4\,C\,mol^{-1}$), and $n$ corresponds to the number of electrons that are transferred in the reaction ($n = 1$ for azurin).

**Redox system.** In our experiments, we have a system consisting of three redox couples:

- Ferricyanide and ferrocyanide,

$$[\mathrm{Fe(CN)_6}]^{3-} + \bar{e} \rightleftharpoons [\mathrm{Fe(CN)_6}]^{4-} \quad (4)$$

- DTT (dithiothreitol) and oxidized DTT,

$$\mathrm{C_4H_{10}O_2S_2} \rightleftharpoons \mathrm{C_4H_8O_2S_2} + 2\mathrm{H^+} + 2\bar{e} \quad (5)$$

- Oxidized azurin $(\mathrm{Az_{ox}})$ and reduced azurin $(\mathrm{Az_{red}})$, ($E_{0,\,\mathrm{Az}} = 21 \pm 19$ mV at pH7, vs SCE)[8]:

$$\mathrm{Az_{ox}} + \bar{e} \rightleftharpoons \mathrm{Az_{red}} \quad (6)$$

At equilibrium, we have the following expression for the redox potential of the system, according to the Nernst equation:

$$E = E_{0,\,\mathrm{FeCN}} - \frac{RT}{F} \ln \frac{[(Fe(CN)_6)^{3-}]}{[(Fe(CN)_6)^{4-}]} = E_{0,\,\mathrm{DTT}} - \frac{RT}{2F} \ln \frac{[DTT_{\mathrm{red}}]}{[DTT_{\mathrm{ox}}]} \quad (7)$$

Thus the redox potential can be calculated if we know the total concentrations of ferri- and ferrocyanide and of oxidized and reduced DTT, or *vice versa*.

Depending on the redox conditions in the sample, an individual azurin molecule will continually switch between the oxidized and the reduced state at a rate which is determined by the concentrations of oxidizing and reducing species. We can evoke the ergodicity principle to formulate the Nernst equation in terms of the population distribution over time in such a two–state model.

The energy difference, $\Delta E$, that is associated with the electron transfer reaction of azurin (Eq. 6), in the presence of the working electrode at a potential $E$ is given by:

$$\Delta E = ne\Delta V = ne(E_0 - E) \tag{8}$$

Here, $e$ is the elementary charge, and $n$ is the number of electrons involved in the reaction, *i.e.* the charge transferred in the reaction is $ne$. Assuming that the time–averaged probabilities for the oxidized and reduced state of azurin, $\bar{P}_{\text{ox}}$ and $\bar{P}_{\text{red}}$, respectively, obey the Boltzmann distribution, we have

$$\frac{\bar{P}_{\text{red}}}{\bar{P}_{\text{ox}}} = e^{ne(E_0 - E)/k_B T} \tag{9}$$

We have just retrieved the Nernst equation (Eq. 3), in terms of $\bar{P}_{\text{ox}}$ and $\bar{P}_{\text{red}}$, as can be seen when we rearrange this equation:

$$E = E_0 - \frac{k_B T}{ze} \ln \frac{\bar{P}_{red}}{\bar{P}_{\text{ox}}} \tag{10}$$

This is clear when it is denoted that $R = k_B \cdot N_A$ and $e = F/N_A$. The only difference is that the concentrations of reduced and oxidized molecules are now replaced by the probabilities of being in either of the two states.

The time–averaged probabilities of being in these states must obey the condition $\bar{P}_{\text{red}} + \bar{P}_{\text{ox}} = 1$. Solving for $\bar{P}_{\text{red}}$ and $\bar{P}_{\text{ox}}$ gives

$$\bar{P}_{\text{red}} = \frac{1}{1 + e^{-\Delta E/k_B T}} \tag{11a}$$

$$\bar{P}_{\text{ox}} = \frac{1}{1 + e^{\Delta E/k_B T}} \tag{11b}$$

If we define the forward and backward rates in Eq. 6 as $k_{\text{red}}$ and $k_{ox}$, respectively, we can also write

$$\frac{k_{ox}}{k_{\text{red}}} = e^{\Delta E / k_B T} \tag{12}$$

If a single molecule, which switches between the two states, is followed for a certain amount of time, we can determine the probability distribution of the dwell times, i.e. the times the molecule stays in either of the two states. For the present case, these distributions are given by[9]

$$P_{\text{ox}}(t) = k_{\text{red}} e^{-k_{\text{red}} t} \tag{13a}$$

$$P_{\text{red}}(t) = k_{\text{ox}} e^{-k_{\text{ox}} t} \tag{13b}$$

We have thus established a firm relationship between redox properties of a single molecule and its dynamic behavior over time.

## Supplementary Experiments:

### FluRedox principle

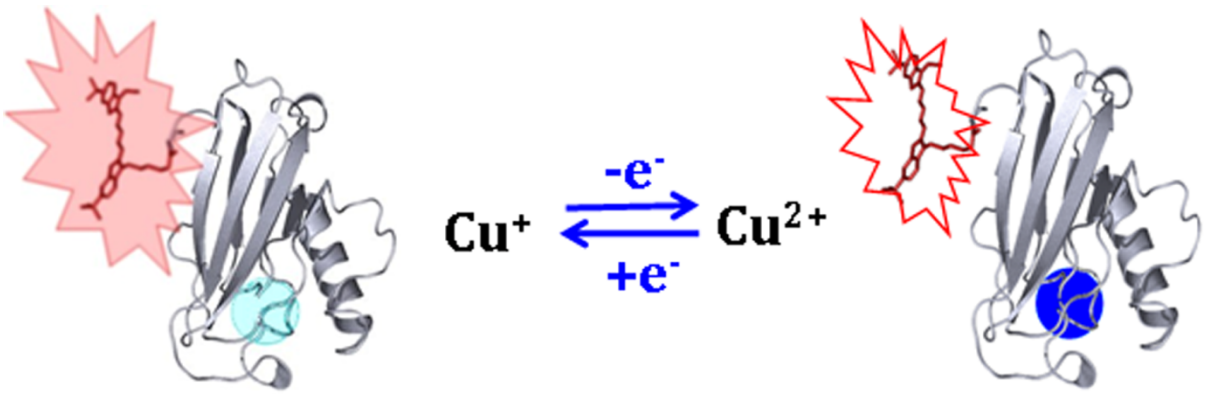


**Fig. S1.** Model of Cy5–NHS labeled wt–azurin based on the crystal structure of wt–azurin by Nar et al.[10] (4AZU.pdb). The label has been attached to the protein via a covalent (amide) bond to the carboxylate group on the dye molecule. The covalently attached Cy5 is excited at a wavelength close to it's extinction maximum, $\lambda_{ex}$. In the reduced form of the protein the Cy5 relaxes by the conventional route, with emission of a photon at a characteristic wavelength, $\lambda_{em}$. In the oxidized form of the protein a FRET process can occur between the excited Cy5 label and the copper redox center (blue sphere), resulting in loss of fluorescence emission.[2,11]

**Absorption spectra of Cu–Az**

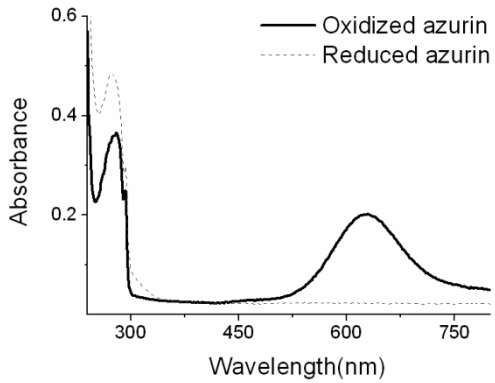


**Fig. S2.** Absorption spectra of Cu–Az in its reduced (dash line) and oxidized (solid line) form. Az absorption spectrum was measured at room temperature 50 μM of Az in 20 mM Hepes buffer solution. The absorption spectrum of oxidized Cu–Az shows two main peaks at 280 nm (tryptophan absorption) and 628 nm ($Cu^{2+}$ absorption). Reduced Cu–Az shows only the 280 nm band.

**Purification of Azurin–Cy5**

In the chromatographic separation in Figure S3A, we have observed multiple peaks because of the variety of labeling sites (exposed lysines) on the azurin surface. From the UV–vis spectral analysis of the eluting species (Fig. S3B), one sees that fraction I shows the same spectrum as the oxidized azurin, which is, therefore, ascribed to unlabeled protein. In this case the band around 628 nm is solely due to the absorption of the $Cu^{2+}$ center, the ratio $Abs_{628nm}/Abs_{280nm}$ ~0.57 being the same as for the native, oxidized protein. The UV–vis spectra of fraction II–IV in Figure S3B display features of the protein as well as the label and are ascribed to singly labeled protein fractions. The spectra show an intense peak around 650 nm accompanied by a shoulder at 600 nm, which indicates the presence of label in the sample. The presence of protein is inferred from two spectral characteristics: the absorption at 280 nm and the typical sharp peak at 291 nm due to the only tryptophan in the sequence. Since we got the highest concentration of the label in fraction II, we used this fraction in all the single molecule experiments. We assume that fraction II is the favorable reaction site of Cy5 NHS–ester with the N–terminus of azurin.[2] Thus, by purification of azurin after labeling with the fluorophore, we avoided immobilization of unlabeled or possible heterogeneously labeled species. Hence, fluorescence decrease is the indication of nonfluorescent dimer formation, when proteins label with multiple amino–reactive Cy5 labels.[12] There are no evidence of that in this work. Moreover, absorption spectrum in Figure S3A does not show any indication of Cy5 dimer formation according to the previous reports.[12,13]

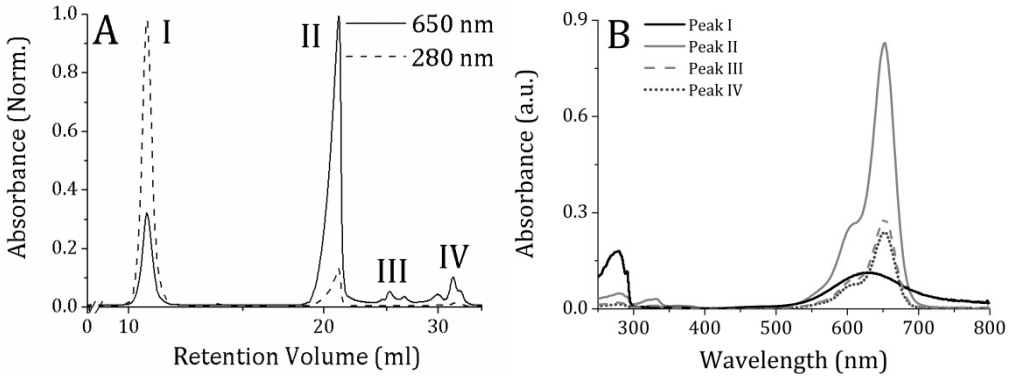

**Fig. S3.** (A) Azurin was labeled with Cy5 and the resulting species were separated with anion exchange chromatography, recording both overall protein absorbance at 280 nm and the specific absorbance of the Cy5 label at 650 nm. (B) Display of the spectra corresponding to the peaks I–IV. The spectra of peaks III and IV strongly overlap, and are almost in distinguishable. The absorbance spectrum of Peak I has the same shape as the UV–Vis absorption spectrum of wt Cu–azurin from *Ps. aeruginosa* in the oxidized form, and is attributed to unlabeled azurin (confirmed by the ratio $Abs_{628nm}/Abs_{280nm}$ of ~0.57, typical of wt azurin). The presence of protein is inferred from two spectral characteristics: the absorption at 280 nm and the typical sharp peak at 291 nm due to the only tryptophan in the sequence.

**Fluorescence intensity traces of Cu–Az/Cy5**

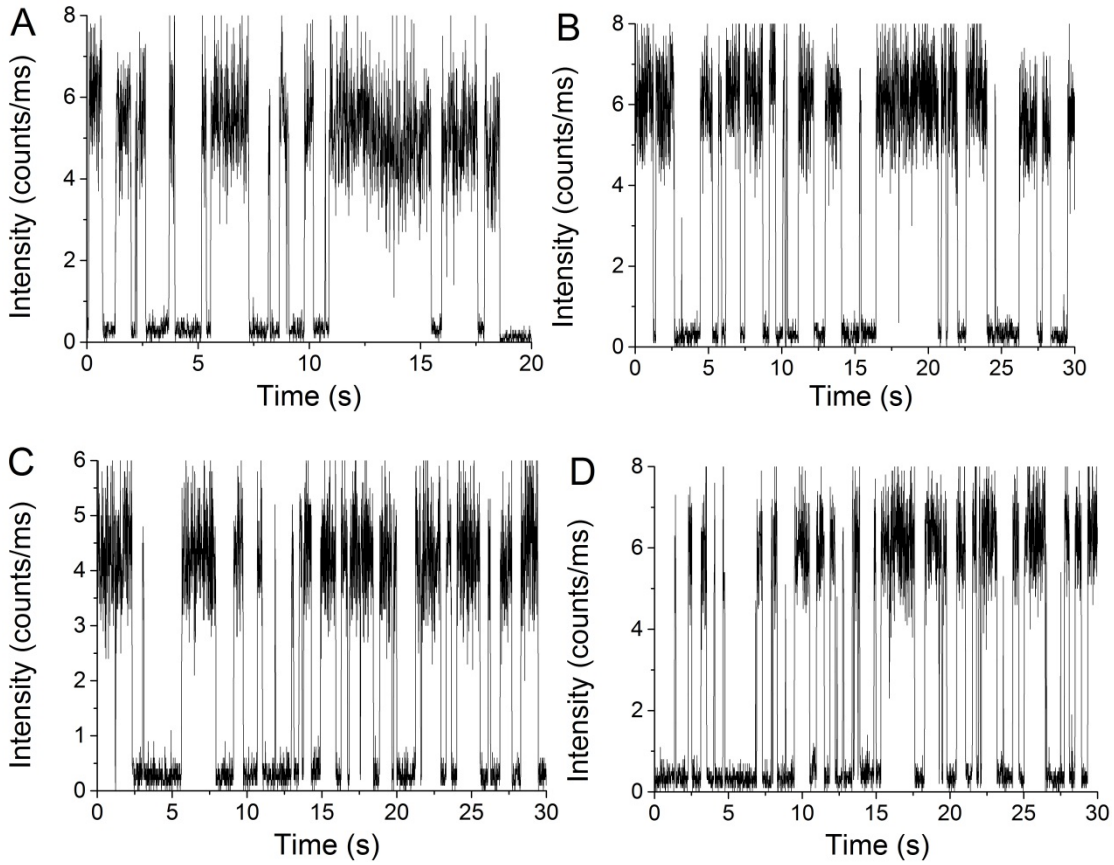

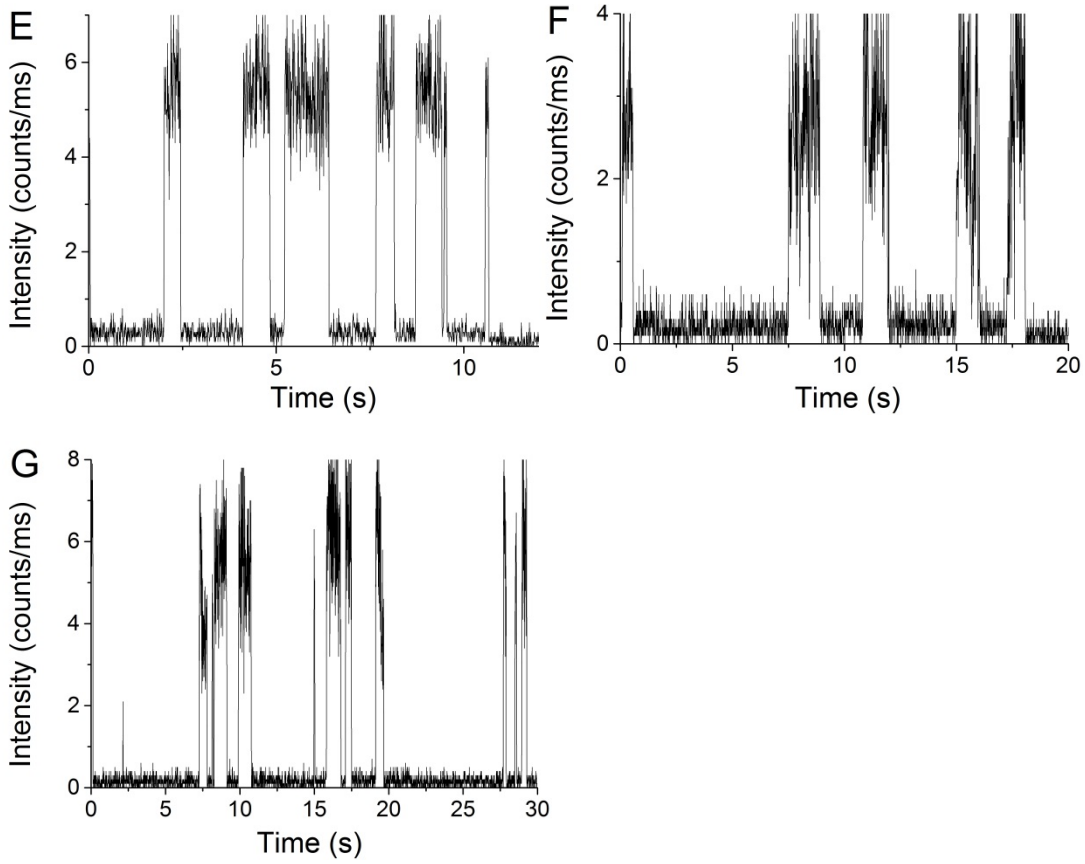


**Fig. S4.** The real time fluorescence intensity traces of a Cy5 labeled single Cu–Az with a 10 ms bin size. The redox potentials ($E$) in solution are (A) −20 mV ($P_{ox}$ = 0.38), (B) 0 mV ($P_{ox}$ = 0.41), (C) 20 mV ($P_{ox}$ = 0.45), (D) 40 mV ($P_{ox}$ = 0.56), (E) 60 mV ($P_{ox}$ = 0.67), (F) 80 mV ($P_{ox}$ = 0.79) and (G) 100 mV ($P_{ox}$ = 0.83) vs SCE.

**Fluorescence intensity traces of Zn–Az/Cy5**

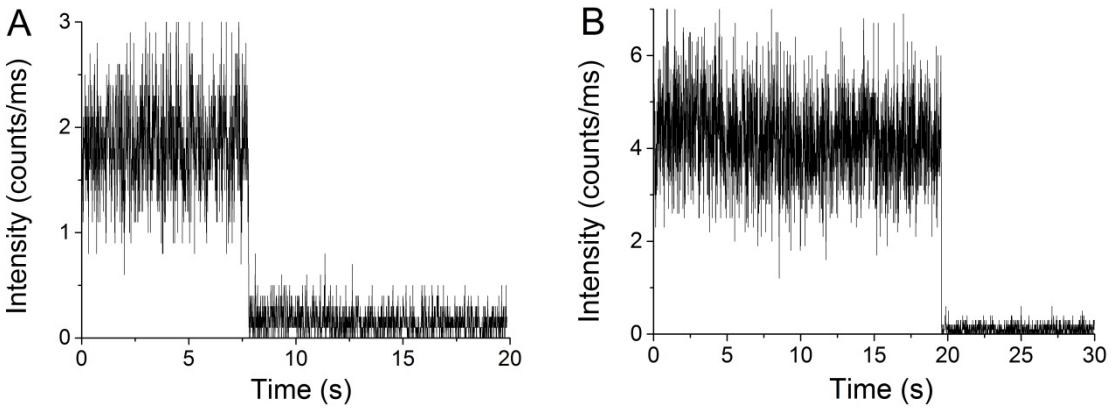


**Fig. S5.** The real time fluorescence intensity traces of a Cy5 labeled single Zn–Az with a 10 ms bin size. The redox potentials ($E$) in solution are (A) 20 mV and (B) 40 mV vs SCE. Zn–Az does not show any fluorescence switching under the same conditions as Cu–Az (Fig. 2 and Fig. S4).

**Fluorescence time courses in bulk**

To verify redox switching in bulk solution, reduction and oxidation of Cy5–labeled azurin was performed by adding reductant (dithiotreitol, DTT) and oxidant (potassium ferricyanide, $K_3(FeCN)_6$) from freshly prepared, concentrated stock solutions (2–20 mM) directly into an optical cuvette to a final concentration of 5–20 µM, *i.e.* in 50 to 200–fold excess. In these experiments, the fluorescence was monitored using a Cary Eclipse Spectrophotometer (Varian Inc., Agilent Technologies, USA). Fluorescence time courses of the labeled protein upon addition of oxidant or reductant were recorded by exciting the sample at 650 nm and monitoring the emission at 685 nm at room temperature in a 3–windows quartz ultra–micro cell with 100 µl total sample volume (Hellma Analytics, Müllheim, Germany). In order to minimize second order diffraction effects of the monochromator gratings suitable optical filters were placed, both, in the excitation and the emission path. The excitation/emission slits were set to 5 nm band-pass. The concentrations of labeled Cu azurin and Cy5 were about 100 nM and Zn azurin was about 50 nM in 100 mM phosphate buffer solution at pH 7.0, respectively.

It is very well known for all the type–1 Cu centres that, while an absorption band is present at 590-630 nm in the $Cu^{2+}$ state, this band is absent in the $Cu^{+}$ state. Thus, one also expects to see a significant resonance energy transfer from the fluorophore to the Cu center in the oxidized but

not in the reduced state of azurin. For instance in Figure S5A (black trace), upon initial addition of oxidant ($K_3(FeCN)_6$), the fluorescence intensity drops due to FRET between the attached fluorophore and the non–fluorescent Cu–center. Subsequent addition of reductant (DTT) produces an increase in the fluorescence intensity. In principle, this redox cycle can be repeated indefinitely as previously reported.[2,11] In fact, the fluorescence intensity in the oxidized state is reduced by about a factor of 10 compared to that in the reduced state in bulk. As a result, we obtained about 90% for the fluorescence-switching ratio (SR) of Az–Cy5. The SR is defined as follows:

$$SR = \frac{I_{RED} - I_{OX}}{I_{RED}} \times 100 \tag{16}$$

where $I_{RED}$ and $I_{OX}$ are the fluorescence intensity values in the reduced bright and oxidized dark state, respectively. Furthermore, Zn–azurin (a redox inactive form of wt azurin, reconstituted with Zn instead of Cu) labeled with Cy5 (grey trace in Fig. S6A) and Cy5 alone (Fig. S6B) was used as a control. They did not show any fluorescence switching upon addition of oxidant or reductant.[14]

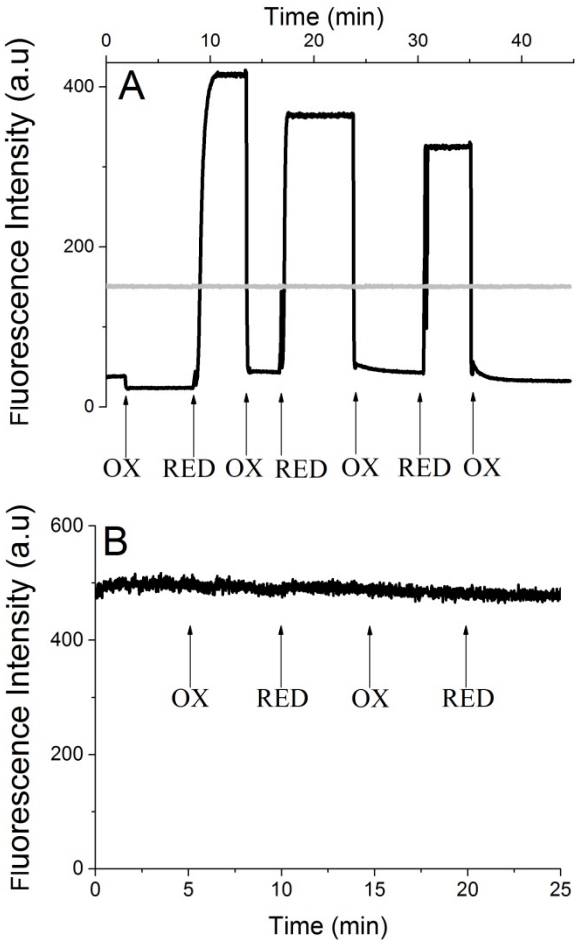


**Fig. S6.** (A) FRET–based on-off switching in bulk. A 100 nM Cy5–labeled Cu–azurin sample was titrated with aliquots of DTT and $K_3(FeCN)_6$ (2 mM) in 100 mM phosphate buffer at pH 7.0. We observed a large, reversible change (black trace) of the fluorescence intensity of Cy5 labeled azurin upon addition of oxidant or reductant. The fluorescence intensity in the oxidized state is reduced by about a factor of 10 compared to that in the reduced state. The gradual decrease starting at the second reduction event is due to the dilution effect. (B) Fluorescence intensity of Cy5 upon addition of oxidant or reductant. Zn–azurin labeled with Cy5 (grey line in Fig. S6A) and Cy5 were used as a control and did not show any fluorescence switch.

**Histograms of midpoint potential ($E_0$) of single azurin molecules**

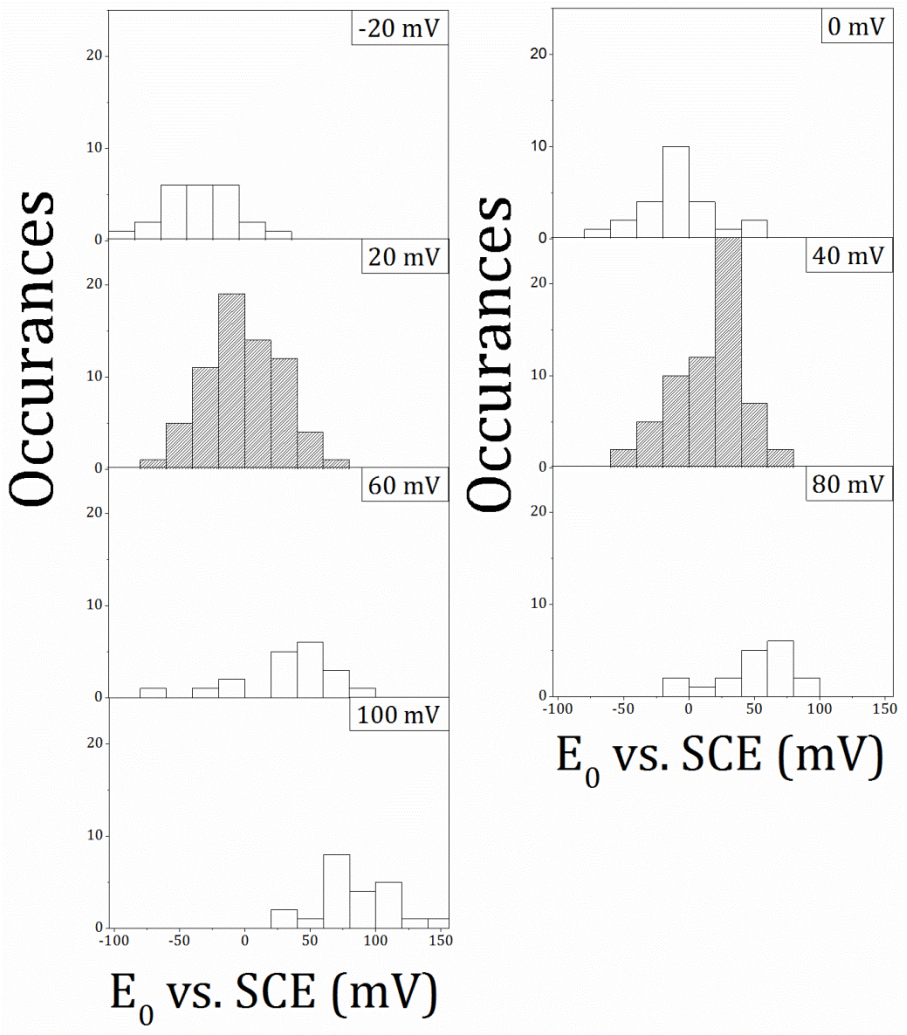


**Fig. S7.** The histograms of midpoint potential ($E_0$) of single azurin molecules at solution potentials ($E$) of −20, 0, 20, 40, 60, 80 and 100 mV. The initial concentration of $K_3[Fe(CN)_6]$ was 200 μM and DTT was added to adjust the redox potential in solution which was measured with a voltmeter using a saturated calomel electrode as a reference and 0.5 mm platinum wire as a counter electrode. All the measurements were performed under anaerobic conditions in a sealed sample–holder under continuous argon flow.

**Rate constants of a single azurin molecule**

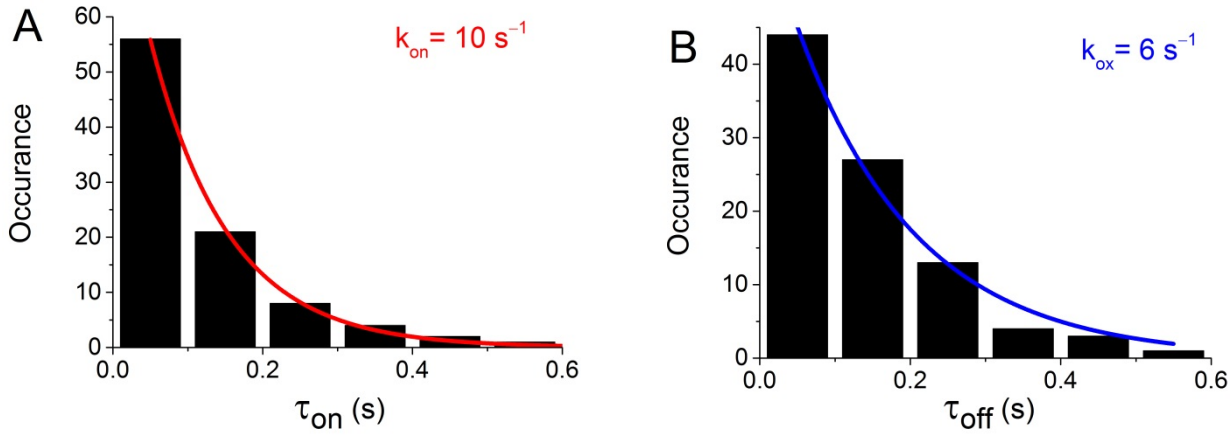


**Fig. S8.** Histograms of (A) on and (B) off times for a single azurin–Cy5 at $E$ = 20 mV. The rate constant is given by the inverse of the characteristic time constants of the mono–exponential fits of the distributions. This result is obtained from the time trace in Figure 2A.

**Fluorescence intensity profile of a single azurin molecule**

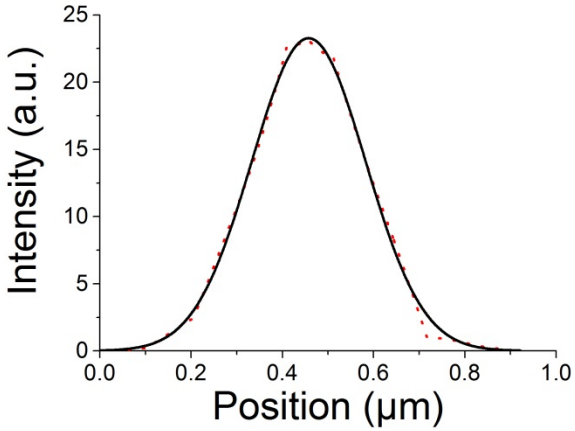

**Fig. S9.** Intensity profile (red dots) taken along the center of a molecule in Figure 1A and fitted with a Gaussian (black solid line). The full–width–at half–maximum (FWHM) is 294 nm, close to the diffraction limited resolution.

**References:**


1. M. van de Kamp, F. C. Hali, N. Rosato, a F. Agro, and G. W. Canters, *Biochim. Biophys. Acta*, 1990, **1019**, 283–92.

2. S. Kuznetsova, G. Zauner, R. Schmauder, O. A. Mayboroda, A. M. Deelder, T. J. Aartsma, and G. W. Canters, *Anal. Biochem.*, 2006, **350**, 52–60.

3. S. Kuznetsova, G. Zauner, T. J. Aartsma, H. Engelkamp, N. Hatzakis, A. E. Rowan, R. J. M. Nolte, P. C. M. Christianen, and G. W. Canters, *Proc. Natl. Acad. Sci. U. S. A.*, 2008, **105**, 3250–5.

4. A. T. Elmalk, J. M. Salverda, L. C. Tabares, G. W. Canters, and T. J. Aartsma, *J. Chem. Phys.*, 2012, **136**, 235101.

5. R. B. Altman, D. S. Terry, Z. Zhou, Q. Zheng, P. Geggier, R. a Kolster, Y. Zhao, J. a Javitch, J. D. Warren, and S. C. Blanchard, *Nat. Methods*, 2012, **9**, 68–71.

6. L. P. Watkins and H. Yang, *J. Phys. Chem. B*, 2005, **109**, 617–28.

7. L. C. Tabares, D. Kostrz, A. Elmalk, A. Andreoni, C. Dennison, T. J. Aartsma, and G. W. Canters, *Chem. A Eur. J.*, 2011, **17**, 12015–9.

8. N. M. Marshall, D. K. Garner, T. D. Wilson, Y.-G. Gao, H. Robinson, M. J. Nilges, and Y. Lu, *Nature*, 2009, **462**, 113–6.

9. P. Nelson, *Biological Physics (Updated Edition)*, W. H. Freeman, 2007.

10. H. Nar, A. Messerschmidt, R. Huber, M. van de Kamp, and G. W. Canters, *J. Mol. Biol.*, 1991, **221**, 765–72.

11. R. Schmauder, S. Alagaratnam, C. Chan, T. Schmidt, G. W. Canters, and T. J. Aartsma, *J. Biol. Inorg. Chem.*, 2005, **10**, 683–7.

12. H. J. Gruber, C. D. Hahn, G. Kada, C. K. Riener, G. S. Harms, W. Ahrer, T. G. Dax, and H.-G. Knaus, *Bioconjug. Chem.*, 2000, **11**, 696–704.

13. U. Schobel, H.-J. Egelhaaf, A. Brecht, D. Oelkrug, and G. Gauglitz, *Bioconjug. Chem.*, 1999, **10**, 1107–1114.

14. J. J. Davis, H. Burgess, G. Zauner, S. Kuznetsova, J. Salverda, T. Aartsma, and G. W. Canters, *J. Phys. Chem. B*, 2006, **110**, 20649–54.